6616 *Chem. Mater.* **2010,** *22,* 6616–6623
DOI:10.1021/cm102122c

CHEMISTRY OF MATERIALS
Article

Intermatrix Synthesis of Polymer−Copper Nanocomposites with Tunable Parameters by Using Copper Comproportionation Reaction

Patricia Ruiz,[†] María Muñoz,[†] Jorge Macanás,[‡] and Dmitri N. Muraviev*[,†]

[†]*Unitat de Química Analítica, Departament de Química, Universitat Autònoma de Barcelona, 08193 Bellaterra, Barcelona, Spain, and* [‡]*Chemical Engineering Department, UPC, Terrassa 08222, Barcelona, Spain*

Received August 30, 2010. Revised Manuscript Received November 17, 2010

This paper describes the synthesis of copper nanoparticles (NPs) inside sulfonated polyetherether ketone (SPEEK) membranes, which serve both as reaction media for intermatrix synthesis (IMS) of Cu-NPs and as stabilizing matrices, preventing NPs aggregation and uncontrollable growth. The IMS technique involves the loading of the functional groups of the polymer with metal ions followed by their reduction inside the polymeric matrix. It has been shown that the repetitive metal loading-reduction cycle, in the case of copper, is accompanied by comproportionation reaction between Cu^0 and Cu^{2+}, leading to the formation of Cu^+ ions. This, in turn, allows for doubling the NPs content in the SPEEK matrix along with the tuning of Cu-NPs size.

Introduction

Synthesis and characterization of metal nanoparticles (MNPs) is one of the hottest topics attracting attention of both scientists and technologists within the past decade and, as a consequence, the preparative methods for synthesis of various MNPs have evolved quite fast. Some of them allows for controlling the size of such nanoparticles and have provided new fundamental insights of the properties of nanoscale materials.[1] Because of their nanometric dimension, both the physical and the chemical properties of MNPs substantially differ from those of respective bulk metals and, in certain instances, these properties can be purposely used to improve the desired characteristics of MNP-containing materials.[2,3] In this context, the synthesis of MNP-containing materials with controllable characteristics is one of the key goals of the modern materials science, which has attracted substantial interest within the recent years.

However, the main drawback of MNPs is their high trend to aggregation, leading to the loss of their specific size and as a consequence, their special properties. Stabilization of MNPs in polymeric matrices is considered to be one of the most promising ways to solve MNPs stability problem and it may help solving some other important issues, such as preventing the uncontrollable growth of MNPs, controlling their size and growth rate, providing MNPs solubility in some organic solvents, and others.[4−11] The intensive development of both the polymer science and the nanoscience and nanotechnology fields has naturally resulted in the appearance of various polymer-based nanocomposites obtained by the incorporation of inorganic particles inside the polymer host matrix. Polymer−metal nanocomposites (PMNCs) containing polymer stabilized metal nanoparticles (PSMNPs)[1,12,13] are examples of the nanocomposite materials of this type, which find numerous applications.[8,14−21]

Copper nanoparticles (Cu-NPs) have been widely used due to their well-known electrocatalytic properties[22] as an

*Corresponding author. E-mail: Dimitri.Muraviev@uab.es.

(1) Sudeep, P. K.; Emrick, T. *ACS Nano* **2009**, *3*(10), 2870–2875.
(2) Schmid, G. *Clusters and Colloids. From Theory to Applications*; VCH: Weinheim, Germany, 1994.
(3) De Jongh, L. J. *Physics and Chemistry of Metal Cluster Compounds*; Kluwer: Dordrecht, The Netherlands, 1994.
(4) Pomogailo, A. D. *Russ. Chem. Rev.* **1997**, *66*(8), 679–716.
(5) Pomogailo, A. D.; Rozenberg, A. S.; Uflyand, I. E. *Metal Nanoparticles in Polymers*; Khimia: Moskow, 2000 (in Russian).
(6) Pomogailo, A. D.; Dzhardimalieva, G. I.; Rozenberg, A. S.; Muraviev, D. N. *J. Nanoparticle Res.* **2003**, *5*(5−6), 497–519.
(7) Muraviev, D. N. *Contrib. Sci.* **2005**, *3*(1), 19–32.
(8) Macanas, J.; Parrondo, J.; Munoz, M.; Alegret, S.; Mijangos, F.; Muraviev, D. N. *Phys. Status Solidi A* **2007**, *204*(6), 1699–1705.
(9) Muraviev, D. N.; Macanas, J; Esplandiu, M. J.; Farre, M.; Muñoz, M.; Alegret, S. *Phys. Status Solidi A* **2007**, *204*(6), 1686–1692.
(10) Corain, B.; Kralik, M. *J. Mol. Catal. A: Chem.* **2000**, *159*(2), 153–162.
(11) Antonietti, M.; Wenz, E.; Bronstein, L.; Seregina, M. *Adv. Mater.* **1995**, *7*(12), 1000–1005.
(12) Keng, P. Y.; Kim, B. Y.; Shim, I.-B.; Sahoo, R.; Veneman, P. E.; Armstrong, N. R.; Yoo, H.; Pemberton, J. E.; Bull, M. M.; Griebel, J. J.; et al. *ACS Nano* **2009**, *3*, 3143–3157.
(13) Macanas, J.; Farre, M.; Muñoz, M.; Alegret, S.; Muraviev, D. N. *Phys. Status Solidi A* **2006**, *203*(6), 1194–1200.
(14) Méli, L.; Green, P. F. *ACS Nano* **2008**, *2*(6), 1305–1312.
(15) Karttunen, M.; Ruuskanen, P.; Pitkänen, V.; Albers, W. A. *J. Electron. Mater.* **2008**, *37*(7), 951–954.
(16) Cioffi, N.; Torsi, L.; Ditaranto, N.; Tantillo, G.; Ghibelli, L.; Sabbatini, L.; Bleve-Zacheo, T.; | D'Alessio, M.; Zambonin, P. G.; Traversa, E. *Chem. Mater.* **2005**, *17*, 5255–5262.
(17) Malinauskas, A.; Malinauskiené, J.; Ramanavicius, A. *Nanotechnology* **2005**, *16*, R51–R62.
(18) Nadagouda, M. N.; Varma, R. S. *Biomacromolecules* **2007**, *8*, 2762–2767.
(19) Reboud, V.; Kehagias, N.; Striccoli, M.; Placido, T.; Panniello, A.; Curri, M. L.; Zelsmann, M.; Reuther, F.; Gruetzner, G.; Sotomayor, C. M. *J. Vac. Sci. Technol., B* **2007**, *25*(6), 2642–2644.
(20) Muraviev, D. N.; Macanas, J.; Farre, M.; Muñoz, M.; Alegret, S. *Sens. Actuators* **2006**, *B118*(1−2), 408–417.
(21) Muraviev, D. N.; Ruiz, P.; Muñoz, M.; Macanás, J. *Pure Appl. Chem.* **2008**, *80*(11), 2425–2437.
(22) Welch, C. M.; Comptom, R. G. *Anal. Bioanal. Chem.* **2006**, *384*, 601–619.

Published on Web 12/06/2010

active component in various electroanalytical applications such as the analysis of carbohydrates,[23] amino acids,[24] nitrite and nitric oxide,[25] and hydrogen peroxide,[26,27] among other compounds.[28,29] Nevertheless, nowadays the electroanalytical applications of MNPs (e.g., in sensors and biosensors) are mainly based on the use of platinum group metals (PGMs) because of their unique catalytic properties. The decrease in the noble metal loading without a remarkable change in the sensitivity of electroanalytical devices is an important challenge for the current technology. The use of core−shell MNPs with a cheap metal core coated with a thin PGMs shell can be a possible strategy to cope with the economical drawback. For this reason, Cu-NPs have also been used as the core in the synthesis of core−shell MNPs by their coating with PGM-shell (such as Pt or Pd),[30−33] which substantially decreases the cost of the final material. In this context, the optimization of the synthesis of both the Cu-core-MNPs and the corresponding polymer−metal nanocomposites is of particular interest.

The use of MNPs in electroanalytical applications is based in many instances on their deposition onto the surface of the corresponding electrochemical devices (e.g., electrode). In case of the PSMNPs, this stage is usually made by dissolution of the polymer−metal nanocomposite in an appropriate solvent followed by deposition of the resulting MNPs solution ("ink") onto the electrode surface and drying to produce a polymer−metal nanocomposite membrane.[7] The initial MNPs concentration in the stabilizing matrix (or the density of MNPs population in the polymer) is the key parameter that permits us to regulate the deposition of the desired number of MNPs per unit area onto the electrode surface.

In this communication, we report the results obtained by studying the conditions of the intermatrix synthesis (IMS)[13,20,32−34] of Cu-NPs in sulfonated poly(etherether ketone) (SPEEK), which permit us to increase the density of NPs population inside the parent polymer. The synthesis of Cu-NPs was carried out by varying the following parameters that influence the IMS process: (i) the reducer concentration, (ii) the copper concentration in the loading solution, and/or (iii) the metal-loading time when using two sequential copper-loading-reduction cycles. It is important to emphasize that the second metal-loading cycle is accompanied by copper comproportionation reaction.[32] This paper reports the first successful application of comproportionation reaction for the IMS of PMNCs with optimal properties (Cu-NPs size and the density of Cu-NPs population in PMNC).

Experimental Methods

Chemicals. Metal salts ($NaBH_4$, $CuSO_4 \cdot 5H_2O$ and others all from Aldrich, Germany), acids, and organic solvents (all from Panreac, S.A. Spain) of p.a. grade were used as received. The polymer (PEEK, Goodfellow) was also used without any pretreatment. Bidistilled water was used in all experiments.

Methods. *Membrane Preparation.* Functionalization (sulfonation) of PEEK was carried out by following the procedure described elsewhere[35,36] by using concentrated sulfuric acid at room temperature. The casting of SPEEK membranes was carried out from a 10% w/w solution of polymer in DMF by using a RK Paint Applicator (K Print Coat Instruments, Ltd.) coupled with temperature controller. The ion-exchange capacity (IEC) of SPEEK membrane was determined by following the procedure described elsewhere[37] and appeared to be about 2 mequiv SO_3^-/g SPEEK in all cases.

Intermatrix Synthesis. The IMS[7,9,13,20,32−34] of Cu-MNPs in SPEEK membranes was carried out by sequential loading the sulfonic groups of the polymer (sulfonic) with Cu^{2+} ions (by using 0.1 M $CuSO_4$ solution) followed by their reduction inside the matrix with aqueous $NaBH_4$ solution (usually 0.5 M).

Instrumentation. The metal content inside SPEEK membranes was determined by using inductively coupled plasma optical emission spectroscopy (ICP-OES, Iris Intrepid II XSP, Thermo Elemental). A sample of around 5 mg of MNP-containing membrane was immersed in 1 mL of aqua regia to completely dissolve copper. The obtained solution was filtrated through a 0.22 μm Millipore filter and adequately diluted for ICP-OES analysis.

The microscopic characterization of Cu-MNPs was carried out by both the transmission electron microscope (TEM, JEOL 2011, Jeol Ltd.) coupled with energy-dispersive spectrometer (R-X EDS INCA) and scanning electron microscope (SEM) (Jeol JSM-6300, Jeol Ltd.) coupled with EDX (LINK ISIS-200, Oxford Instruments). Samples of Cu-MNP-SPEEK composite membranes were dissolved in DMF and resulting suspensions (MNP-inks) were used for TEM analysis. A drop of diluted ($\sim$ 20 times) MNP-ink was deposited on a grid followed by evaporation of the solvent under ambient conditions. To carry out the characterization of a cross-section of the Cu-PSMNPs-SPEEK by TEM or SEM techniques, the solid nanocomposites were first immobilized in epoxy resin an then frozen at low temperature (−160 °C) followed by their sectioning with a Leica EM UC6 Ultramicrotome using a 35° diamond knife (Diatome).

MNPs size distribution were determined by converting enlarged TEM images into Adobe Acrobat Reader files followed by the measurement of the particle diameters by using the object measurement tool of the software (around 400 NPs were measured). Each histogram of MNPs size distribution was fitted with a 3 parameter Gaussian function (see equation below), where x_0 corresponds to an average diameter corresponding to

(23) Male, K. B.; Hrapovic, S.; Liu, Y.; Wang, D.; Luong, J. H. T. *Anal. Chim. Acta* **2004**, *516*, 35–41.
(24) Zen, J.-M.; Hsu, C.-T.; Kumar, A. S.; Lyuu, H.-J.; Lin, K.-Y. *Analyst* **2004**, *129*, 841–845.
(25) Wang, H.; Huang, Y.; Tan, Z.; Hu, X. *Anal. Chim. Acta* **2004**, *526*, 13–17.
(26) Zen, J.-M.; Chung, H.-H.; Kumar, A. S. *Analyst* **2000**, *125*, 1633–1637.
(27) Somasundrum, M.; Kirtikara, K.; Tanticharoen, M. *Anal. Chim. Acta* **1996**, *319*(1−2), 59–70.
(28) Zen, J.-M.; Song, Y.-S.; Chung, H.-H.; Hsu, C. T.; Kumar, A. S. *Anal. Chem.* **2002**, *74*, 6126–6130.
(29) Zen, J.-M.; Chung, H.-H.; Kumar, A. S. *Anal. Chem.* **2002**, *74*, 1202–1206.
(30) Zhong, C.-J.; Maye, M. M. *Adv. Mater.* **2001**, *13*(19), 1507–1511.
(31) Zhou, S.; Varughese, B.; Eichhorn, B.; Jackson, G.; McIlwrath, K. *Angew. Chem., Int. Ed.* **2005**, *44*, 4539.
(32) Muraviev, D. N.; Macanas, J.; Parrondo, J.; Muñoz, M.; Alonso, A.; Alegret, S.; Ortueta, M.; Mijangos, F. *React. Funct. Polym.* **2007**, *67*(12), 1612–1621.
(33) Muraviev, D. N.; Ruiz, P.; Muñoz, M. *Phys. Status Solidi A* **2008**, *205*(6), 1460–1464.
(34) Kickelbick, G. *Prog. Polym. Sci.* **2003**, *28*(1), 83–114.
(35) Linkous, C. A.; Anderson, H. R.; Kopitzke, R. W.; Nelson, G. L. *Int. J. Hydrogen Energy* **1998**, *23*(7), 525–529.
(36) González-Bellavista, A.; Macanás, J.; Muñoz, M.; Fàbregas, E. *Sens. Actuators, B* **2006**, *115*(2), 691–696.
(37) Zhao, C.; Li, X.; Wang, Z.; Dou, Z.; Zhong, S.; Na, H. *J. Membr. Sci.* **2006**, *280*, 643–650.

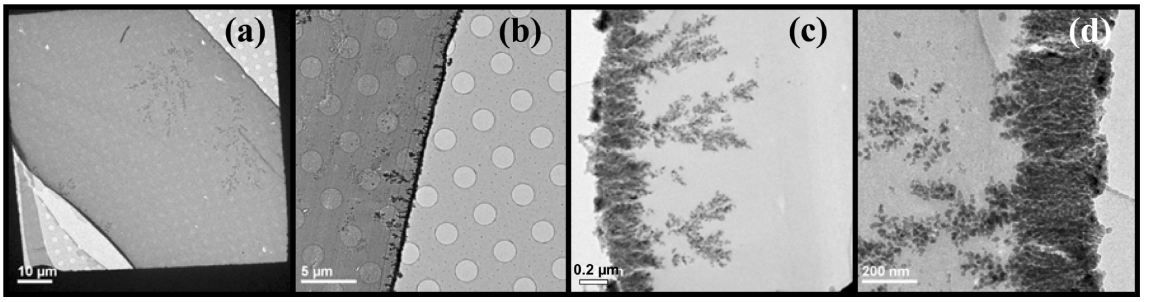

Figure 1. TEM images of the same SPEEK-Cu-PSMNP membrane sample cross-section with different magnification (d > c > b > a).

the highest fraction of nanoparticles and σ is the standard deviation.

$$y = a\exp\left[-0.5\left(\frac{(x-x_0)}{\sigma}\right)^2\right]$$

Results and Discussion

Intermatrix Synthesis of Cu-NPs: First Metal-Loading Reduction Cycle. IMS of Cu-NPs inside the SPEEK membrane can be described schematically by the following two-steps procedure: (1) the loading of membrane with Cu^{2+} (eq 1) ions followed by (2) the reduction of Cu^{2+} to Cu^0 with $NaBH_4$ (eq 2).

$$2R\text{-}SO_3^-Na^+ + Cu^{2+} \rightleftarrows (R\text{-}SO_3^-)_2Cu^{2+} + 2Na^+ \quad (1)$$

$$(R\text{-}SO_3^-)_2Cu^{2+} + 2NaBH_4 + 6H_2O \rightarrow 2R\text{-}SO_3^-Na^+ + 7H_2(g) + 2B(OH)_3 + Cu^0(s) \quad (2)$$

As is seen, the loading step (eq 1) is based on a simple ion-exchange process between copper and sodium cations. The second IMS stage, which corresponds to the reduction reaction (eq 2), is in fact the sum of reactions 3 and 4. The polymeric membrane serves as a sort of a nanoreactor because IMS of MNPs proceeds inside the polymeric matrix. The formation of Cu-NPs is preceded by the ion-exchange reaction (eq 3), which corresponds to the inverse reaction of 1. This reaction gives raise to the flux of Cu^{2+} ions directed to the membrane surface, where they are reduced to zerovalent state by the borohydride anions. The Cu-NPs formation (see eq 4) shifts the ion-exchange equilibrium in reaction 3 to the right what results in the complete displacement of divalent ions (Cu^{2+}) with monovalent ones (Na^+) from the functional groups, although this contradicts to the "normal" affinity of the polymer (which is higher toward double-charged ions in comparison with monocharged ones). For this reason, the functional sulfonic groups of the polymer appear to be completely regenerated (converted back into the initial Na-form). A similar situation is observed in other ion-exchange systems where the ion-exchange reaction is coupled with a solid phase formation.[38]

$$(R\text{-}SO_3^-)_2Cu^{2+} + 2Na^+ \rightleftarrows 2R\text{-}SO_3^-Na^+ + Cu^{2+} \quad (3)$$

$$Cu^{2+} + 2BH_4^- + 6H_2O \rightarrow 7H_2(g) + 2B(OH)_3 + Cu^0(s) \quad (4)$$

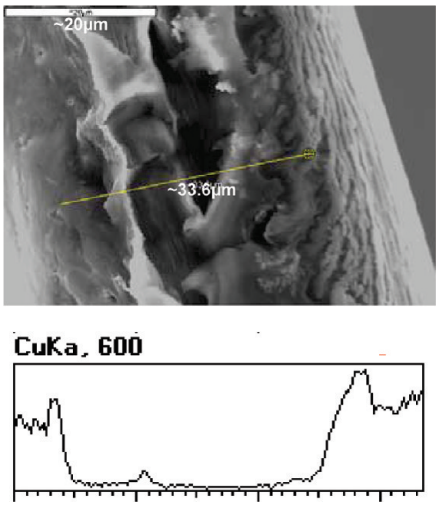

Figure 2. (a) SEM image and (b) Cu concentration profile obtained by EDX for to a SPEEK-Cu-PSMNP membrane cross-section. EDX profile corresponds to the ~33.6 μm line indicated in the SEM image.

As is clearly seen from eqs 3 and 4 and follows from the above discussion, the IMS of MNPs results not only in the formation of NPs in the polymer but also in the complete regeneration of its functional groups. Therefore, the polymer can repeatedly undergo an additional metal loading-reduction cycle with the same metal ion (for example, to accumulate more MNPs in the polymer) or with another one. In the last case, MNPs obtained after the first metal-loading-reduction cycles appear to be coated with the second metal what results in the formation of bimetallic MNPs with core−shell structure. The characterization of Cu-PSMNP-SPEEK nanocomposites by various microscopic techniques (TEM and SEM) testifies that the sulfonic groups of the polymer are not blocked by MNPs as the major part of Cu-NPs are accumulated near the membrane surface forming fractals with "treelike" structure (see Figure 1). Copper concentration profile along the nanocomposite membrane cross-section obtained by SEM coupled with EDX is in agreement with this conclusion (Figure 2). These results allow for better understanding the mechanism of MNPs formation in the course of IMS. In fact, borhydride anions cannot deeply penetrate in the negatively charged polymer matrix due to the Donnan exclusion effect.[39−42] Therefore, Cu^{2+} ions

(38) Helfrich, F. *Ion Exchange*; McGraw-Hill: New York, 1962.
(39) Donnan, F. G. *J. Membr. Sci.* **1995**, *100*(1), 45–55.
(40) Cumbal, L.; Sengupta, A. K. *Environ. Sci. Technol.* **2005**, *39*(17), 6508–6515.
(41) Helfferich, F. *Ion Exchange*; Dover Publications: New York, 1995.

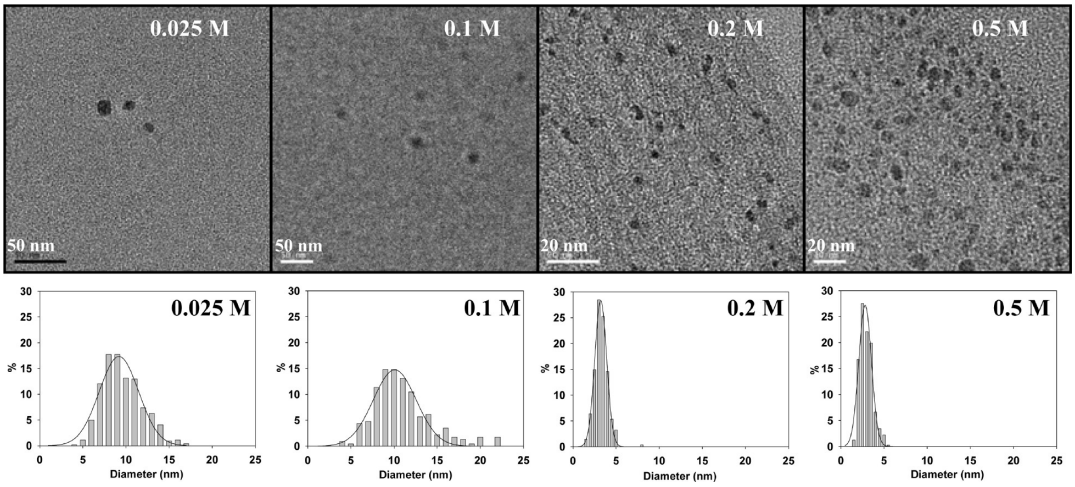

Figure 3. TEM images and size distribution histograms of Cu-PSMNPs obtained by using $NaBH_4$ solution of different concentrations.

displaced from the functional groups can only be reduced to Cu^0 when they come in contact with borohydride anions near the membrane surface. Although after IMS the MNPs are mainly located on the surface of the membrane, the dissolution of PMNC in an appropriate solvent (e.g., DMF) followed by the second membrane casting has been shown to result in a homogeneous distribution of MNPs in the nanocomposite.[43] It seems also important to emphasize that dissolution of nanocomposite membranes does not lead to any aggregation of MNPs (see Figure 3), which testifies to the quite good stabilizing ability of SPEEK matrix toward PSMNPs.

The possibility to easily produce PMNCs with different distributions of MNPs is of great importance as it allows for maximally tuning the properties of nanocomposites to their further applications. For example, in catalytic applications, the best situation is when the catalysts MNPs are located near the polymer surface what provides the maximum accessibility of the reactants to the catalytic centers. In electrochemical or electroanalytical applications (e.g., in sensors and biosensors), a homogeneous distribution of MNPs has been considered to be preferable as it enhances the electroconductivity of PMNC membrane (by the electron hopping mechanism[44]). However, our recently published results[43,45] have demonstrated the influence of the MNPs distribution on some important sensor parameters, such as the sensitivity and the response time. The same conclusion also follows from the results reported by other authors.[46,47]

The kinetics of IMS in the case of SPEEK (or any other ion-exchange membrane[41]) is determined by the following stages:

Table 1. Results of ICP-OES Analysis and Histogram Parameters (see 3 parameter Gaussian function equation) of Cu-MNP-SPEEK Membranes after One Metal-Loading-Reduction Cycle

$[NaBH_4]$ (M)	mg Cu/g SPEEK	d_m (nm)	σ (nm)	R^2
0.025	46.4 ± 0.3	9.2	2.3	0.945
0.1	44.4 ± 0.1	10.1	2.5	0.949
0.2	46.4 ± 0.3	3.2	0.7	0.992
0.5	47.0 ± 0.4	2.8	0.7	0.947

(1) diffusion of Na^+ ions inside the membrane to the functional groups (occupied by Cu^+ ions);

(2) ion-exchange reaction of displacement of Cu^{2+} with Na^+ ions;

(3) diffusion of Cu^{2+} ions to the periphery of membrane;

(4) reduction of Cu^{2+} ions to Cu^0 by borohydride anions (reaction 4).

Ion diffusion across the membrane (stage 3) can be considered as the rate-determining step of the IMS process. It seems clear that the rate of this process depends on the initial concentration of borohydride (or Na^+ ions) in the external solution, as the rate of diffusion is known to depend on the concentration gradient of the diffusing species. On the other hand, the rate of reaction 4, which also depends on the concentration of Cu^{2+} ions (and borohydride anion concentration), determines the conditions of MNPs formation and their growth. From this, one can suggest that the reduction of Cu^{2+} ions with $NaBH_4$ solution of different concentrations has to result in the formation of MNPs with different sizes (diameters). This hypothesis is supported by the results collected in Table 1. Is it is seen that the increase in the reducer concentration in external solution leads to a decrease in the diameter of Cu-NPs formed, although the total copper content in the nanocomposite membrane remains essentially the same (see Figure 3). This also results in the formation of MNPs with a more narrow size distribution (see Figure 3 and respective σ values in Table 1). In this series of experiments, Cu-PSMNPs were synthesized by carrying out one metal-loading-reduction cycle in SPEEK membranes of the same weight (19.02 ± 0.08 mg) and using different $NaBH_4$ concentrations. Note that similar results have

(42) Dorfner, K. *Ion Exchangers*; Walter der Gruyter Publishers: Berlin, 1991.
(43) Ruiz, P.; Muñoz, M.; Macanás, J.; Turta, C.; Prodius, D.; Muraviev, D. N. *Dalton Trans.* **2010**, *39*(7), 1751–1757.
(44) Ruffino, F.; Piro, A. M.; Piccitto, G.; Grimaldi, M. G.; Bongiorno, C.; Spinella, C. *Appl. Phys. A: Mater. Sci. Process.* **2009**, *97*, 63–72.
(45) Alonso, A.; Macanas, J.; Shafir, A.; Muñoz, M.; Vallribera, A.; Prodius, D.; Melnic, S.; Turta, C.; Muraviev, D. N. *Dalton Trans.* **2010**, *39*(10), 2579–2586.
(46) Kang, X.; Mai, Z.; Zou, X.; Cai; Mo, , J. *Anal. Biochem.* **2007**, *363*, 143–150.
(47) Li, L.-H.; Zhang, W.-D. *Microchim. Acta* **2008**, *163*, 305–311.

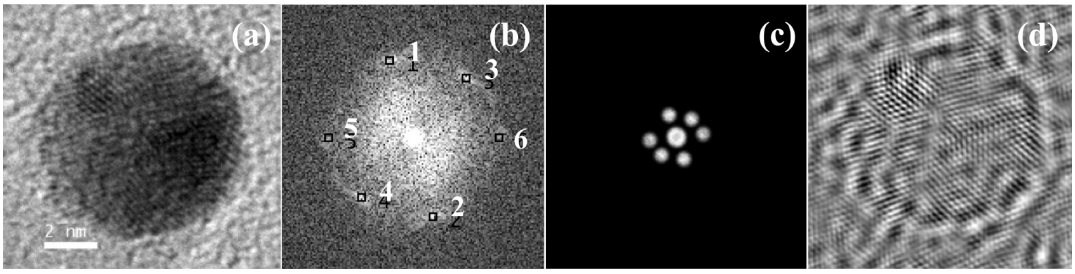

Figure 4. Results of TEM analysis of Cu-PSMNPs obtained by IMS technique: (a) HRTEM image of Cu-NP; (b) diffraction pattern of Cu-PSMNP shown in (a); (c) diffraction pattern shown in b after FFT treatment by applying a mask; and (d) Cu-NP image obtained by inverse FFT.

been reported for the other types of MNPs synthesized by the chemical reduction, such as, for example, gold nanoparticles.[48−52]

The results of the microscopic analysis of Cu-NPs synthesized by using one metal-loading-reduction cycles and reduced with 0.2 M $NaBH_4$ are shown in Figure 4. As follows from images a and b in Figure 4, Cu-NPs in all cases are characterized by a clear crystalline structure (each couple of diffraction points in Figure 4b indicates the crystallographic planes of the copper nanocrystal). The use of the fast Fourier transform (FFT) analysis of the diffraction pattern shown in Figure 4a permits us to quantitatively confirm the above qualitative conclusion. The copper crystallographic plane distances obtained by FFT analysis were determined to be 0.2304, 0.2258, 0.2308, 0.2306, 0.2151, and 0.2111 nm, respectively (for points 1−6, respectively, see Figure 4b). These values are in a good agreement with the crystallographic data of copper metal.[53]

Because membrane thickness normally influences the rate of ion diffusion through the membrane, it was worth analyzing if this parameter could play a role in the IMS of Cu-MNPs. Table 2 shows the Cu content in Cu-NPs prepared by a single metal-loading-reduction cycle in SPEEK membranes with different thicknesses (where IEC corresponds to 2.01 ± 0.04 meq SO_3^-/g SPEEK). In spite of the above assumption, it is seen that membrane thickness within a sufficiently wide range (0.011−0.155 mm) does not essentially influence the Cu-NP content in the nanocomposite.

Intermatrix Synthesis of Cu-MNPs by Using Two Sequential Metal-Loading-Reduction Cycles. As has already been suggested above, after the first metal-loading-reduction cycle and Cu-NP formation the sulfonic groups of the polymer are regenerated allowing for carrying out the second cycle. In the case of copper, one can expect oxidation of Cu-NPs preformed within the first cycle by Cu^{2+} ions of the second metal-loading solution what has

Table 2. ICP-OES Analysis of Cu-NP-SPEEK Membranes after First Metal-Loading-Reduction Cycle

membrane thickness (mm)	mg Cu/mequiv SO_3^-
0.011	26.6 ± 0.08
0.016	23.5 ± 0.2
0.019	27.5 ± 0.06
0.027	29.0 ± 0.11
0.036	26.9 ± 0.05
0.05	30.1 ± 0.05
0.07	28.6 ± 0.02
0.155	29.7 ± 0.02

to result in the formation of Cu^+ ions. This hypothesis is based on the strong negative shift of the oxidation−reduction potential ($E°$) of Cu-NPs in comparison with that of the bulk copper.[54] In other words, Cu-NPs are far stronger reducers and if this supposition is valid, the following comproportionation reaction has to proceed inside the membrane in the course of the second metal loading

$$Cu^0 + Cu^{2+} \rightarrow 2Cu^+ \quad (5)$$

If the above redox reaction (eq 5) takes place, each functional group of the polymer appears to be occupied by the monovalent copper ion (eq 6). Therefore, the total amount of copper inside SPEEK membrane after reduction with sodium borohydride solution (eq 7) has to be as twice as high in comparison with that obtained after the first metal-loading-reduction cycle. This conclusion clearly follows from the comparison of eq 7 with eq 2:

$$R\text{-}SO_3^-Na^+ + Cu^+ \rightarrow R\text{-}SO_3^-Cu^+ + Na^+ \quad (6)$$

$$2R\text{-}SO_3^-Cu^+ + 2NaBH_4 + 6H_2O \rightarrow 2R\text{-}SO_3^-Na^+ + 7H_2 + 2B(OH)_3 + 2Cu^0 \quad (7)$$

Note that eq 7 refers solely to the copper case because of its unique chemical properties, whereas eq 6 can be written in a general form for any metal ion.

The qualitative confirmation of the above supposition can be observed in Figure 5, where the light photographs of SPEEK membranes after different stages of the IMS process are shown. The initial translucent SPEEK membrane (see Figure 5a) changes its color to bright cupric metallic (see Figure 5b) after the first metal loading-reduction cycle. Within the second metal-loading process (immersion of the

(48) Turkevich, J.; Stevenson, P. C.; Hillier, J. *Faraday Discuss.* **1951**, *11*, 55–75.
(49) Mohamed, M. B.; Wang, Z. L.; El-Sayed, M. A. *J. Phys. Chem. A* **1999**, *103*(49), 10255–10259.
(50) Murray, B. S.; Dickinson, E.; McCarney, J. M.; Nelson, P. V.; Whittle, M. *Langmuir* **1998**, *14*(13), 3466–3469.
(51) Teranishi, T.; Miyake, M. *Chem. Mater.* **1998**, *10*(2), 594–600.
(52) Teranishi, T.; Hosoe, M.; Tanaka, T.; Miyake, M. *J. Phys. Chem. B* **1999**, *103*(19), 3818–3827.
(53) Powder Diffraction File; JCPDS-International Centre for Diffraction Data: Newtown Square, PA, 1998.
(54) Plieth, W. J. *J. Phys. Chem.* **1982**, *86*(16), 3166–70.

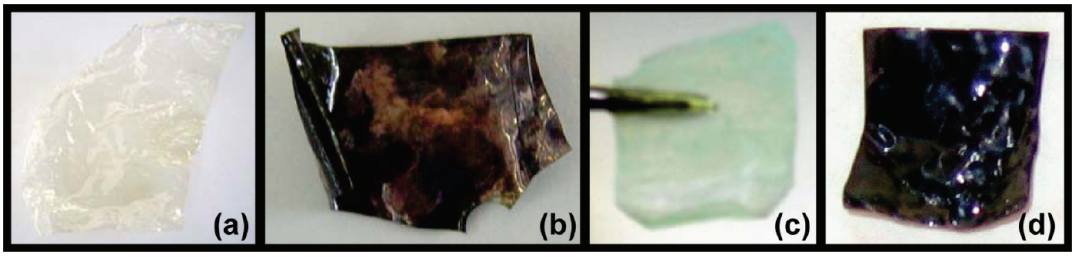

Figure 5. Light images corresponding to (a) SPEEK membrane, (b) SPEEK-Cu-PSMNPs nanocomposite membrane after first metal-loading-reduction cycle, (c) same membrane after second metal loading, and (d) after second metal-reduction cycle.

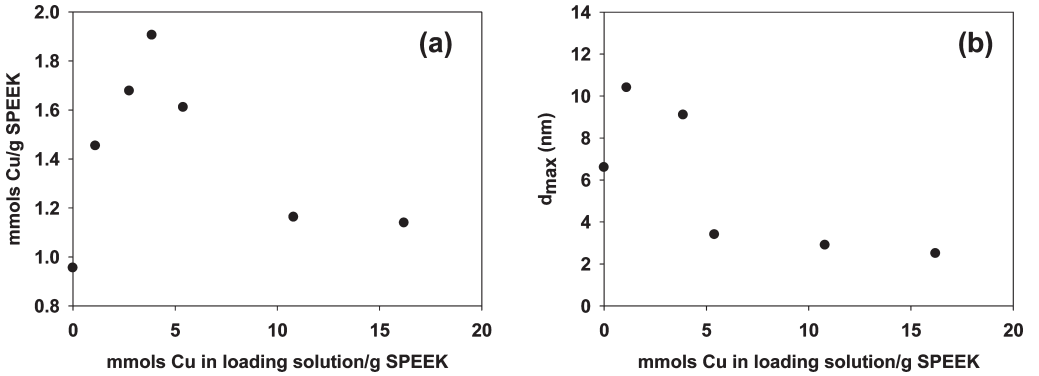

Figure 6. (a) Total content of Cu-PSMNPs inside membrane samples and (b) average diameter of Cu-PSMNPs vs $[Cu^{2+}]$ in the second cycle-loading solution.

membrane shown in Figure 5b in Cu^{2+} solution), the bright metallic color of the membrane completely disappears. It becomes again translucent with a greenish color, which is typical for the Cu(I) salts (Figures 5c). Finally, after the second metal reduction with $NaBH_4$, the membrane takes again the metallic color, which intensity is higher than that after the first cycle (Figure 5d).

Influence of $[Cu^{2+}]$ in Second Metal-Loading Solution. To better understand the above phenomenon, a series of experiments was carried out by changing $[Cu^{2+}]$ in the second metal loading solution. The results of the measurements of both the total copper content per gram of membrane and the diameter of Cu-NPs in the nanocomposites are shown in Figure 6. As is seen in Figure 6a, the gradual increase of $[Cu^{2+}]$ in the second loading solution results in the increase of total copper content inside the membrane until it achieves the maximum, the value of which is twice as high in comparison to the initial copper content (obtained after the first cycle). This point corresponds to the complete comproportionation of Cu^0 and Cu^{2+} (see eq 5). A further increase in $[Cu^{2+}]$ in the second loading solution should also favor the comproportionation reaction, but as can be seen in the same figure, a higher $[Cu^{2+}]$ leads to a decrease in Cu-NP content inside the membrane; at a significant excess of copper in the second loading solution, the composition of the PMNC membrane appears to be quite similar to that obtained after the first metal-loading-reduction cycle. The reason of this effect is the displacement of Cu^+ ions by Cu^{2+} from the functional groups of the polymer (see eq 8), which is favored by the higher concentration of Cu^{2+} ions as well as by the higher affinity of sulfonic groups toward divalent ions versus monovalent ones.[41,42] As a result, the functional groups of the polymer appear to be occupied by Cu^{2+} because of the complete displacement of both Na^+ and Cu^+ ions (eqs 1 and 8). In other words, the situation becomes similar to what is observed after the first metal-loading cycle. That is why the final metal reduction gives a similar Cu-NP content in the nanocomposite membrane.

$$2\text{R-SO}_3^-\,\text{Cu}^+ + \text{Cu}^{2+} \rightarrow (\text{R-SO}_3^-)_2\text{Cu}^{2+} + 2\text{Cu}^+ \quad (8)$$

As it follows from the results of the measurements of Cu-NP diameters in PMNC samples shown in Figure 6b, the diameters of Cu-NPs obtained at low $[Cu^{2+}]$ are higher than those obtained at a higher copper concentration in the second loading solution. This fact can be explained as follows:

(1) A low copper concentration cannot provide a complete oxidation of all Cu^0 and, as a consequence, Cu-NPs remaining inside the membrane serve as nucleation centers for the reduced Cu^0, which appears within the second metal-reduction cycle. In this case, MNP growth proceeds by the heterogeneous crystallization mechanism, and their diameters gradually increase.

(2) A higher copper concentration results in the complete oxidation of Cu^0 by Cu^{2+} ions to Cu^+ and further formation of new Cu-NPs occurs by the homogeneous crystallization mechanism, which is most probably the reason for their smaller size in comparison to the previous case.

Although the total copper content per gram of PMNC sample (determined by ICP-OES analysis) and Cu-NP size distribution (obtained by the analysis of TEM images) are the only experimentally measurable parameters

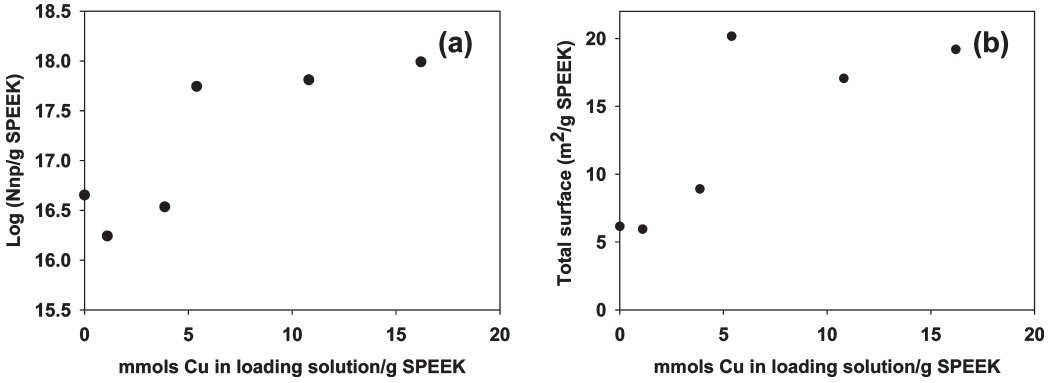

Figure 7. Results of calculations of (a) N_{np} and (b) S_{np} for different PMNC samples (see Figure 6).

of the system, their combination makes it possible to estimate the specific surface area of MNPs obtained (S_{TOTAL}), which is an important parameter in various practical applications of PMNCs such as, for example, heterogeneous catalysis and also electrocatalysis. This estimation can be done by using eqs 9 and 10 and assuming that MNPs are of spherical shape. The results of these calculations are shown in Figure 7.

$$N_{np} = m_{Cu}/\rho_{Cu}(4/3\pi r_{Cu}{}^3) \quad (9)$$

$$S_{TOTAL} = N_{np}S_{np} = N_{np}4\pi r_{Cu}{}^2 = N_{np}\pi d_{Cu}{}^2 \quad (10)$$

Here N_{np} is the total number of MNPs per gram of PMNC, m_{Cu} is the mass of Cu-NPs per gram of PMNC, ρ_{Cu} is the density of copper metal, r_{Cu} is the most frequent radius of Cu-NPs, S_{np} is the surface area of one MNP, $S_{TOTAL} = S_{np}N_{np}$ and $d_{Cu} = 2r_{Cu}$.

Figure 7a shows that N_{np} value increases for samples prepared by using a more concentrated copper solution, which can be explained considering that the mean size, volume, and the mass of the formed Cu-NPs is smaller. On the other hand, S_{TOTAL} parameter appears to be almost constant for samples prepared by using the second metal loading solution with copper concentration higher than ~5 mmol/g SPEEK even when the total amount of copper is lower for these samples (Figure 7b). Again, the ruling parameter in this case is the mean size of Cu-NPs.

Influence of Time of Second Metal Loading. In all the above experiments, the second metal loading was carried out during a fixed time interval of 24 h. However, the contact time of preformed Cu-NPs and Cu^{2+} ions of the second metal-loading solution can be another important parameter, which may influence the conditions of Cu-NPs formation. Comproportionation reaction between preformed Cu-NPs and Cu^{2+} ions is a heterogeneous process and the kinetics of such processes is usually not as fast as the corresponding homogeneous ones. Hence, the contact time can also be used as a parameter for the tailored "tuning" of PMNCs properties.

The experiments described in this section were carried out by using a new set of SPEEK samples with lower ion-exchange capacity (1.81 ± 0.04 mequiv SO_3^-/g SPEEK), which were characterized by the maximum copper loading (similar to that shown in Figure 6) at the concentration of the second loading solution corresponding to 1.6 mmol Cu/g SPEEK. This concentration was used as a fixed value to perform the second metal-loading stage at different contact times (from 0 to 300 min). In all cases, after the second metal loading, the samples were rinsed with water and then reduced with 0.5 M $NaBH_4$ solution.

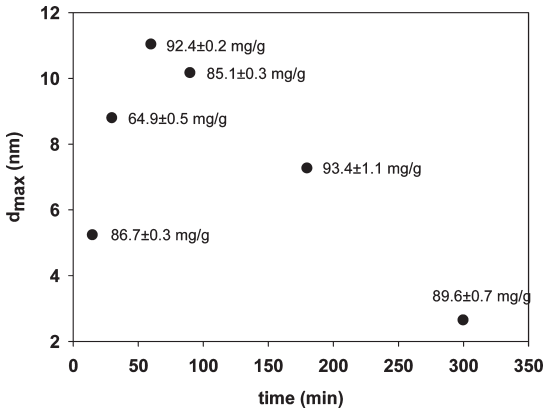

Figure 8. Average diameters for Cu-PSMNPs obtained by a second loading-reduction cycle vs different metal-loading times.

The results of this series of experiments are shown in Figure 8, where the dependence of MNP diameters on the time of second metal loading is shown. The numbers near each point indicate the total copper content (mg Cu/g SPEEK) in each PMNC sample.

As is seen, at low contact time values (< 60 min), the diameter of MNPs gradually increases and then reaches a maximum. The further increase of the contact time results in an almost linear decrease of MNP diameters. These results can be explained similarly to those reported above (see comments to Figure 6b):

(1) At contact times < 60 min, the comproportionation reaction between Cu-NPs and Cu^{2+} ions proceeds incompletely, and the further crystallization of copper proceeds onto the remaining nanoparticles serving as the nucleation centers.

(2) At longer contact times, comproportionation results in the complete disappearance of Cu-NPs and the second crystallization of copper proceeds by the homogeneous mechanism resulting in the formation of smaller Cu-NPs. The decrease in MNP diameters can be probably explained by the Cu^+:Cu^{2+} ratio in the membrane prior

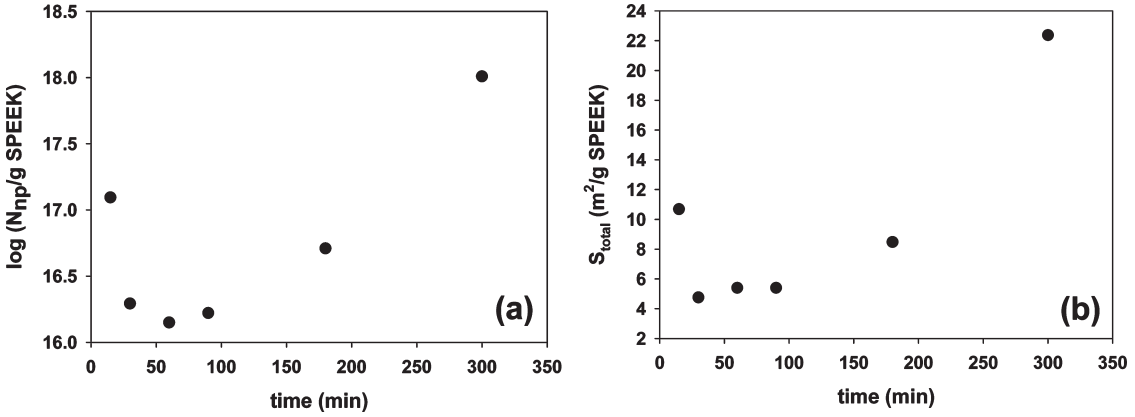

Figure 9. Results of calculations of (a) N_{np} and (b) S_{np} for different PMNC samples (see Figure 8).

to the second copper reduction. However, this point requires additional experimental confirmation.

It seems interesting to note that in the first case the MNPs growth follow the "bottom-up" scenario while in the second case it changes to the "top-down" one. A similar trend is observed when applying different copper concentrations as the tuning parameter of the system.

The results of calculations of N_{np} and S_{TOTAL} parameters (see eqs 9 and 10) from the data shown in Figure 8 are presented in Figure 9. When comparing the data from Figures 7 and 9, one can conclude that the general trend of changes in both N_{np} and S_{TOTAL} by using both tuning parameters (either $[Cu^{2+}]$ in the second metal-loading solution or contact time) is quite similar. This means that both of them can be used as variable for the tailored IMS of Cu-NP-based PMNCs with the desired set of properties by applying the comproportionation reaction as the main tuning tool. It also seems important to note that as also follows from the results of the last series of experiments, the increase in the total amount of Cu-NPs in the PMNC can be achieved within a quite short period of time (far less than 24 h). In conclusion, it seems important to emphasize that this paper reports the first successful application of IMS technique coupled with comproportionation reaction for the synthesis of PMNCs with easily tunable parameters. In the case of this new version of IMS technique, the polymeric membrane can be considered as the real nanoreactor because the comproportionation reaction can proceed only between Cu-PSMNPs and Cu^{2+} ions diffusing from the external solution to the reaction site.

Conclusions

The results reported in this paper demonstrate that the synthesis of Cu-PSMNPs in functional polymer (SPEEK) can be easily carried out by using the IMS technique, which consists in the loading of the functional groups with metal ions following by their reduction inside the polymer matrix. When using IMS of PSMNPs process, the nature and the concentration of the reducing agent plays an active role in the case of sodium borohydride, both cation and anion actively participate in the IMS process. Thus, sodium cations replace previously loaded copper ions (Cu-MNP precusors) from the functional groups of the polymer, whereas the negatively charged borohydride anions serve as the reducing agents and determine the distribution of PSMNPs inside the matrix. Moreover, different MNPs diameters can be obtained by varying the reducer concentration.

The IMS technique gives a unique possibility to carry out sequential metal-loading-reduction cycles what permits in the case of copper to couple it with the comproportionation reaction between preformed Cu-MNPs and Cu^{2+} ions of the second metal loading solution. This in turn gives a chance to double under certain conditions the density of MNPs population in the polymer. Several system parameters such as, the concentration of the second metal loading solution and the time of the second metal loading, can be used for tunning the key properties (diameter of Cu-MNPs and the total copper content in the polymer) of the final polymer−metal nanocomposite. The likelihood to successfully carry out the comproportionation reaction between Cu-MNPs and Cu^{2+} ions is determined by the strong negative shift of redox potential of the former in comparison with bulk copper metal. Stabilization of Cu-NPs by the polymer plays the key role in this case, as it prevents their aggregation and loss as a result of the unique properties. In this context, the results obtained can be considered as the first experimental confirmation of the strong change of reducing ability of MNPs in comparison with respective bulk metals. Finaly, the synthesis of Cu-PSMNPs has a great importance because copper is a cheap catalytically active metal and can be used as a catalyst in many applications. On the other hand, Cu-MNPs can serve as a core to synthesize low-cost PGM-containing core−shell nanocatalysts. In both cases, optimization of the IMS of Cu-PSMNPs as well as the key parameters of nanocomposite materials on their base is of particular importance.

Acknowledgment. This work was supported by the research grant MAT2006-03745, 2006-2009 from the Ministry of Science and Innovation of Spain. J. Macanás thanks the support of Departament d'Innovació, Universitats i Empresa, for a postdoctoral grant. Special thanks are given to Servei de Microscopia from Universitat Autònoma de Barcelona.